



Experimental and Computational Study on Molecular Structure and Vibrational Analysis of Hydroxybenzopyridine Using DFT Method

RUBARANI P. GANGADHARAN¹ and S. SAMPATH KRISHNAN^{2,*}

¹Department of Physics, Rajalakshmi Engineering College, Thandalam, Chennai-602 105, India

²Department of Applied Physics, Sri Venkateswara College of Engineering, Chennai-602 105, India

*Corresponding author: E-mail: sambathk@svce.ac.in

Received: 29 July 2013;

Accepted: 12 December 2013;

Published online: 16 July 2014;

AJC-15527

The experimental and theoretical vibrational spectra of hydroxybenzopyridine were investigated. The experimental FT-IR and FT-Raman spectra of the molecule in the powder form were recorded. Theoretical vibrational frequencies and geometric parameters (bond lengths and bond angles) were calculated using density functional B3LYP method with 6-31G(d,p) basis sets by Gaussian program, for the first time. The complete assignments were performed on the basis of the potential energy distribution of the vibrational modes, calculated with scaled quantum mechanical method. The formation of the hydrogen bond was investigated using natural bond orbital (NBO) calculations. The electron density-based local reactivity descriptors such as Fukui functions were calculated. The calculated HOMO and LUMO energies show that charge transfer occur within the molecule. The dipole moment (μ) and polarizability (α), anisotropy polarizability ($\Delta\alpha$) and first order hyperpolarizability (β_{total}) of the molecule have been reported.

Keywords: FTIR, FT-Raman, DFT, Natural bond orbital.

INTRODUCTION

Hydroxybenzopyridine also called as 8-hydroxy quinoline is an organic compound with the formula C_9H_7NO . It is a derivative of the heterocyclic quinoline by placement of an OH group on carbon number 8. This light yellow compound is widely used commercially, although under a variety of names. It is usually prepared from quinoline-8-sulfonic acid and from a Skraup synthesis from 2-aminophenol¹. 1-Azanaphthalene-8-ol is a monoprotic bidentate chelating agent. Related ligands are the Schiff bases derived from salicylaldehyde such as salicylaloxine, salen and salicylaldehyde isonicotinoyl-hydrazene (SIH). The complexes as well as the heterocyclic itself exhibit antiseptic, disinfectant and pesticide properties², functioning as a transcription inhibitor. Its solution in alcohol is used as liquid bandages. It once was of interest as anti cancer drug. An antiseptic with mild fungistatic, bacteriostatic, anthelmintic and amebicidal action. It is also used as a reagent and metal chelator, as a carrier for Radio-Indium for diagnostic purposes and its halogenated derivatives are used in addition as Topical Anti-Infective Agents and oral antiamebics.

The reaction of hydroxybenzopyridine with aluminum(III)³ results in Alq₃, a common component of organic light emitting diodes (OLED's). Hydroxybenzo-pyridine and its derivatives are widely used as chelating reagents in analytical chemistry

and radiochemistry from metal ion extraction and fluometric determination⁴.

Hydroxybenzopyridine are well known because can perform as structurally related subunits in important bimolecular and biochemical process, which shows strong cytotoxic and antimicrobial properties and they represent the main component in some bactericide, fungicide and antimalarial drugs^{5,6}. Experimentally it was found that hydroxybenzopyridine has analogous properties such as an intense fluorescence in concentrated acids, lack of fluorescence in water or alkenes or formation of the hydrogen bonded clusters with water, ammonium or alcohol molecules Literature survey reveals that to the best of our knowledge, the results based on quantum chemical calculations, vibrational spectral studies and HOMO-LUMO analyses on hydroxybenzopyridine have no reports.

In this study molecular geometry, optimized parameters and vibrational frequencies are computed and the performance of the computational methods for B3LYP at 6-31G(d,p) basis sets are compared. These methods predict relatively accurate molecular structure and vibrational spectra with moderate computational effort. In particular for polyatomic molecules the DFT methods lead to the prediction of more accurate molecular structure and vibrational frequencies than the conventional *ab initio* Hartree-Fock calculations. Among DFT calculation, Beck's three parameter hybrids functional combined with the

Lee-Yang-Parr correlation functional (B3LYP) is the best predicting results for molecular geometry and vibrational wave numbers for moderately larger molecule^{7,8}.

EXPERIMENTAL

The fine polycrystalline of hydroxybenzopyridine was purchased from Sigma-Aldrich Chemical Company with a stated purity 97 % and it was used as such without further purification. The FTIR spectrum of molecule was recorded in the region 4000–450 cm^{-1} on a Perkin Elmer FTIR BX spectrometer calibrated using polystyrene bands. FT-Raman spectrum of the sample was recorded using 1064 nm line of Nd:YAG laser as excitation wave length in the region 1000–5000 cm^{-1} on a Bruker RFS 100/S FT-Raman spectrometer. Liquid nitrogen cooled Gediode was used as a detector. Spectra were collected for samples with 1000 scan accumulated for over 30 min duration. The spectral resolution after apodization was 4 cm^{-1} . A correction according to the fourth power scattering factor was performed, but no instrumental correction was done.

Computational details: In order to obtain stable structures, the geometrical parameters of hydroxybenzopyridine in the ground state was optimized at DFT-B3LYP level of theory using 6-31G(d,p) basis set. There are no significant differences between geometric and vibrational frequencies by the selection of the different basis sets. The calculated vibrational frequencies are scaled by 0.961 for B3LYP/6-31G(d,p)⁹. For B3LYP with 6-31G(d,p) basis set, the wave numbers in the ranges from 4000 to 100 cm^{-1} are scaled with 0.963¹⁰. The molecular geometry was not restricted and all the calculations (vibrational wave numbers, geometric parameters and other molecular properties) were performed by using Gauss View molecular visualization program¹¹.

All calculations were carried out with the Gaussian 03 package¹². The calculations of systems contain C,H,N and O is described by the standard 6-31G(d,p) basis set function of the density functional theory (DFT)^{13,14}. Geometry optimization was performed utilizing Becker's hybrid three-parameter exchange functional and the nonlocal correlation functional of Lee, Yang and Parr (B3LYP)¹⁵. Vibrational analysis was performed at each stationary point found, that confirm its identity as an energy minimum. The population analysis has also been performed by the natural bond orbital method¹⁶ at B3LYP/6-31G(d,p) level of theory using NBO program¹⁷ under Gaussian 03 program package.

RESULTS AND DISCUSSION

Geometric structure: The molecular structure of hydroxybenzopyridine belongs to C1 point group symmetry. The optimized molecular structure of title molecule is obtained from Gaussian 03 and Gauss view 05 program. The labeling of atoms in hydroxybenzopyridine is given in Fig. 1. The optimized geometrical parameters (bond lengths and angles) calculated by B3LYP with 6-311G++(d,p) and cc-pVDZ basis sets are listed in Table-1. The calculated C-C bond length of the ring varied such as C2-C3, C3-C4, C4-C5, C5-C6, C5-C10, C6-C7, C7-C8, C8-C9, C9-C10. But the bond length of C3-C4 and C6-C7 well coincides, calculated by B3LYP method with 6-31G++(d,p) and cc-pVDZ basis sets. The calculated bond

TABLE-1
OPTIMIZED GEOMETRIC PARAMETERS OF HYDROXYBENZOPYRIDINE BY B3LYP AND cc-pVDZ METHODS

Parameter	Method/basis set		
	B3LYP/6-31G++(d p)	cc-pVDZ	exp ^a
Bond length(Å)			
N(1)-C(2)	1.316	1.321	1.346
N(1)-C(10)	1.358	1.361	1.402
C(2)-C(3)	1.414	1.418	1.390
C(2)-H(12)	1.086	1.095	
C(3)-C(4)	1.374	1.379	1.360
C(3)-H(13)	1.083	1.091	
C(4)-C(5)	1.416	1.421	1.422
C(4)-H(14)	1.085	1.093	
C(5)-C(6)	1.417	1.421	1.408
C(5)-C(10)	1.424	1.427	1.409
C(6)-C(7)	1.376	1.381	1.363
C(6)-H(15)	1.084	1.092	
C(7)-C(8)	1.412	1.416	1.393
C(7)-H(16)	1.084	1.093	
C(8)-C(9)	1.397	1.383	1.355
C(8)-H(17)	1.083	1.091	
C(9)-C(10)	1.428	1.433	1.410
C(9)-O(11)	1.35	1.348	1.352
O(11)-H	0.974	0.981	1.420
Bond angle (°)			
C(2)-N(1)-C(10)	118.09	117.79	120.4
N(1)-C(2)-C(3)	123.17	123.26	121.0
N(1)-C(2)-H(12)	116.73	116.68	
C(3)-C(2)-H(12)	120.07	120.04	
C(2)-C(3)-C(4)	119.14	119.18	120.9
C(2)-C(3)-H(13)	119.6	119.63	
C(4)-C(3)-H(13)	121.24	121.17	
C(3)-C(4)-C(5)	119.74	119.67	119.6
C(3)-C(4)-H(14)	120.83	120.87	
C(5)-C(4)-H(14)	119.42	119.44	
C(4)-C(5)-C(6)	124.5	120.75	122.2
C(4)-C(5)-C(10)	116.27	116.16	118.7
C(6)-C(5)-C(10)	119.21	119.07	119.1
C(5)-C(6)-C(7)	119.55	119.53	119.4
C(5)-C(6)-H(15)	119.53	119.53	
C(7)-C(6)-H(15)	120.9	120.94	
C(6)-C(7)-C(8)	121.76	121.92	121.4
C(6)-C(7)-H(16)	119.67	119.58	
C(8)-C(7)-H(16)	118.55	118.49	
C(7)-C(8)-C(9)	119.88	119.80	120.8
C(7)-C(8)-H(17)	120.8	120.96	
C(9)-C(8)-H(17)	119.31	119.23	
C(8)-C(9)-C(10)	119.86	119.63	119.4
C(8)-C(9)-O(11)	121.5	122.18	119.9
C(10)-C(9)-O(11)	118.63	118.18	120.7
N(1)-C(10)-C(5)	123.56	123.90	119.4
N(1)-C(10)-C(9)	116.71	116.05	120.7
C(5)-C(10)-C(9)	119.71	120.03	119.9
C(9)-O(11)-H	106.0	104.38	100

^aTaken from Ref. [45]

length of C=O (1.35 Å) is in good agreement with the experimental value and C-H bond length are slightly differed from it. The O-H bond distance is very small compared than all other bond lengths of the hydroxybenzopyridine.

The density functional calculation gives the very high bond angle of N1-C2-C3 (123°17'). The C-C-C angle is constant which is found to be 119° of this compound. The electron donating substituents on the benzene ring, the symmetry of the ring is distorted, yielding ring angles smaller than 120°

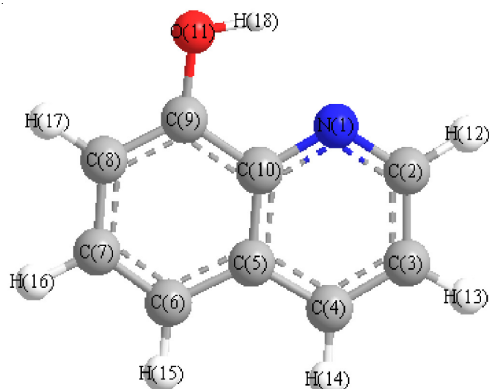


Fig. 1 The atom numbering system for hydroxybenzopyridine

at the point of substitution and slightly larger than 120° at the *ortho* and *meta*-positions¹⁸. The C9-O11-H18 bond gives very small angle 106° . The variation in bond angle depends on the electro negativity of the central atom, the presence of lone pair of electrons and the conjugation of the double bonds. If the electro negativity of the central atom decreases, the bond angle decreases. Further the results of our calculations, the experimental and calculated geometric parameters agree well with remaining geometrical parameters. The small deviations are probably due to the intermolecular interactions in the crystalline state of the molecule.

Vibrational analysis: The vibrational spectral assignments of hydroxybenzopyridine have been carried out with the help of potential energy distribution analysis. The internal coordinates describe the position of the atoms in terms of distances, angles with respect to an origin atom. In this study, the full sets of 70 standard internal coordinates for title compound were defined as given in Table-2. The experimental FT-IR and FT-Raman spectra are shown in Figs. 2 and 4, respectively. For a comparative purpose the calculated IR and Raman spectra with 6-31G(d,p) basis sets are shown in Figs. 3 and 5, respectively. The scaled calculated harmonic vibrational frequencies at B3LYP levels, observed vibrational frequencies and detailed potential energy distribution (PED) assignments are tabulated in Table-3. To our best of knowledge, there are no theoretical studies on the vibrational assignments of hydroxy-

TABLE-2 DEFINITION OF INTERNAL COORDINATES OF HYDROXYBENZOPYRIDINE		
No.	Type	Definition
Stretching		
1-6	C-H	C2-H12,C3-H13,C4-H14,C6-H15,C7-H16,C8-H17
7-15	C-C	C2-C3,C3-C4,C4-C5,C5-C10,C10-C9,C9-C8,C8-C7,C6-C7,C5-C6
16-17	C-N	C2-N1,C10-N1
18	C-O	C9-O11
19	O-H	O11-H18
Bending		
20-25	Ring 1	C3-C2-N1,C2-N1-C10,N1-C10-C5,C5-C4-C3,C10-C5-C4,C4-C3-C2
26-31	Ring 2	C5-C10-C9,C10-C9-C8,C9-C8-C7,C8-C7-C6,C7-C6-C5,C6-C5-C10
32-42	C-C-H	C2-C3-H13,C3-C2-H12,C3-C4-H14,C4-C3-H13,C5-C4-H14,C5-C6-H15,C7-C6-H16,C8-C7-H16,C7-C8-H17,C9-C8-H17
43-44	C-C-O	C8-C9-O11,C10-C9-O11
45	C-O-H	C9-O11-H18
46-47	C-C-N	C3-C2-N1,C5-C10-N1
48	C-N-C	C2-N1-C10
Out of Plane		
49-54	C-H	C2-C2-H12-N1,C2-C3-H13-C4,C3-C4-C5-H14,C5-C6-H15-C7,C6-C7-C8-H16,C9-C8-C7-H17
55-56	C-O	C10-C9-C8-O11,C10-C9-O11-H18
Torsion		
57-62	Ring 1	C3-C2-N1-C10,C2-N1-C10-C5,N1-C10-C5-C4,C10-C5-C4-C3,C5-C4-C3-C2,C4-C3-C2-N1
63-68	Ring 2	C5-C10-C9-C8,C10-C9-C8-C7,C9-C2-C7-C6,C8-C7-C6-C5,C7-C6-C5-C10,C6-C5-C10-C9
69-70	Butterfly	N1-C10-C5-C6,C9-C10-C5-C4

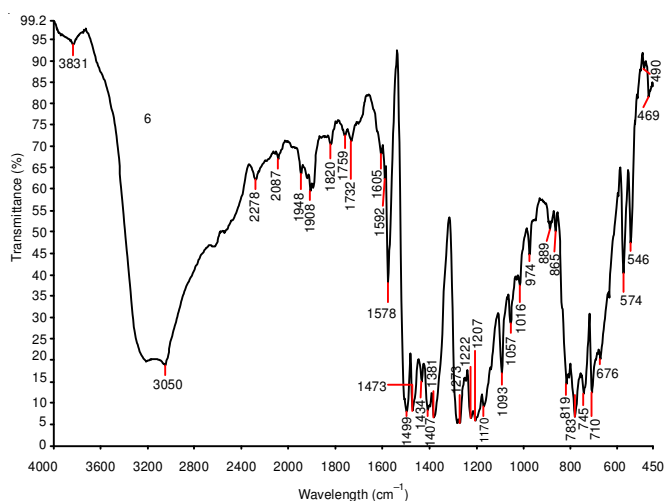


Fig. 2. Experimental FT-IR spectrum of hydroxybenzopyridine B3LYP/6-31G(d,p)

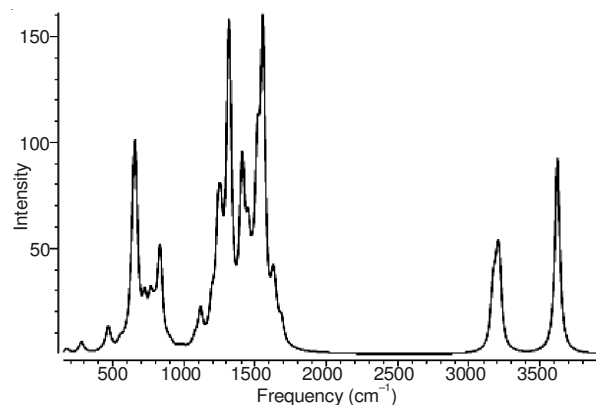


Fig. 3. Comparative graph of calculated IR spectra

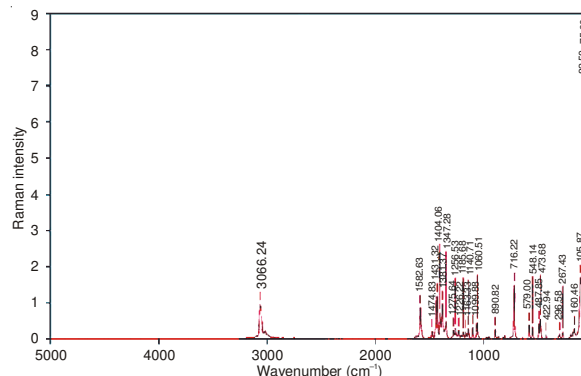


Fig. 4. Experimental FT-Raman spectrum of title molecule B3LYP/6-31G(d,p)

TABLE-3
OBSERVED FT-IR, FT-RAMAN AND CALCULATED WAVE NUMBERS USING B3LYP METHOD WITH 6-31G(d,p)
AND 6-311++G(d,p) BASIS SETS AND PROBABLE ASSIGNMENTS FOR HYDROXYBENZOPYRIDINE

Mode No.	Observed frequencies (cm ⁻¹)		Calculated frequencies (cm ⁻¹)				Vibrational assignments (>10 % PED)
	FT-IR	FT-Raman	B3LYP/6-31G(d,p)		B3LYP/6-311++G(d,p)		
			Scaled	Unscaled	Scaled	Unscaled	
1	3831s		3482	3620	3506	3645	vC2H(97)
2	3190w		3094	3217	3075	3197	vC3H(73) vC4H(22)
3			3088	3210	3070	3192	vC7H(86) vC6H(10)
4			3078	3200	3062	3183	vC5H(62) vC6H(14) vC4H(11)
5	3066s		3063	3184	3048	3168	vC4H(66) vC3H(17) vC5H(10)
6			3062	3183	3044	3165	vC6H(71) vC5H(25)
7			3046	3167	3030	3150	vOH(96)
8	3050w		1621	1686	1605	1669	vC7C8(28) δOH(21)
9	1650s		1586	1649	1570	1632	vC5C6(21) vC9C10(11)
10	1605s	1582s	1567	1629	1550	1612	vC3C4(27) vC4C10(14) vC2N(16)
11	1592s		1495	1555	1480	1538	δOH(21) vC3C4(11) vC7C6(13)
12	1578w	1474w	1459	1517	1444	1501	δOH(25) vC2C3(13) vC5C6(15)
13	1550vs	1431vs	1425	1482	1412	1468	δC6H(16) δC5H(13) vC8O(10) δC2H(10) vC5C10(10)
14	1499vw	1381vs	1396	1452	1383	1438	δC2H(25) δC3H(17) vC4C10(11)
15	1478w		1361	1415	1347	1400	vC9C10(35) vC5C10(12)
16	1381vw		1352	1406	1334	1387	vC9C8(15) vC7C8(13)
17	1350s	1275s	1266	1317	1255	1305	vC8O(13) δC5H(11) vC2N(10) δC4H(10)
18	1275vw	1256s	1244	1314	1246	1295	vC2N(22) δC7H(18) vC8O(10)
19	1222w	1226s	1212	1260	1202	1250	vC4C10(20) vC5C10(16) δC6H(13)
20	1207w	1185s	1192	1240	1182	1229	δC5H(20) δC6H(13) δC3H(12) δC4H(12)
21	1170w	1163s	1151	1197	1146	1191	δC3H(77)δC7H(17)δC2H(12) δC6H(10)
22	1150s		1119	1164	1113	1158	δC4H(15) δC5H(12) vC3C4(10)
23	1093w	1099s	1074	1117	1069	1111	vC2C3(22) δC2H(14) vC7C6(11)C3C4(10)
24	1057w	1060s	1037	1079	1031	1072	vC4C10(11) δC3H(10) vC8O(10) δC6H(10)
25			1012	1053	1006	1046	vC7C6(21) vC2C3(11) vC5C6(11) δring 5(11)
26	1016s		958	996	956	994	γC6H(74) γC5H(19) γC7H(17)
27	974s		936	974	939	976	γC3H(60) γC4H(44)
28			924	961	922	959	γOH(89)
29	889s	890w	870	905	869	903	γC2H(45) γC4H(21) γC5H(11) γOH(10)
30	865s		855	889	856	890	γC7H(52) γC5H(22) γC2H(21)
31	819w		801	833	796	828	δ ring 2(24) δring 5(18)
32	783vw		787	819	788	819	γC2H(21) γC3H(15) γC5H(13) γC4H(11) γC7H(11)
33	745w		762	793	766	796	δring 5(28) δ ring 2(17) δring 6(11) δring 3(11) vC9N(10)
34	710w		737	967	732	761	γC5H(40) γC4H(16) γC6H(15) γC3H(11)
35	676s		697	725	694	722	τ ring 5(37) τ ring 2(32) γC8O(11)
36		716s	633	659	622	647	vC9C8(10)
37			618	643	596	620	τring 5(38) τ ring 2(21)
38	574s	579s	569	592	565	588	γC8O(35) butterfly(21) τ ring 2(18) τ ring 6(10)
39			564	587	564	587	vC9C10(21) δ ring 4(11)
40	546s	548s	532	554	533	554	δring 1(40) δ ring 4(22) δ ring 6(15) δ ring 3(11)
41		487s	479	498	479	498	δring 1(22) δ ring 3(20)
42	490s	473s	458	477	455	474	γC8O(17) τ ring 6(17) τ ring 3(17) τ ring 2(15) τ ring 5(12)
43	469s		451	469	451	469	δ ring 4(37) δ C8O(16) δ ring 3(14)
44		422w	415	432	411	428	τ ring 4(53) τ ring 3(41)
45		296vw	271	282	269	279	δ ring 6(21) δ C8O(21)
46		267s	260	271	257	267	Butterfly(35)γC8O(16) τ ring 6(14)
47		160s	171	178	169	176	τ ring 1(54) τ ring 4(21) τ ring 6(20)
48		105vs	150	156	145	151	τ ring 6(42) butterfly(32) τ ring 1(28)

Abbreviations: s-strong; vs-very strong; ms-medium strong; w-weak; vw-very weak; γ-stretching; β- bending; ω-wagging; τ-Torsion

benzopyridine in the literature. So, in order to introduce detailed vibrational assignments of hydroxybenzopyridine, we have performed computational analysis done by using potential energy distribution analysis and the visualization of modes.

Computed IR intensity and raman activity analysis: Computed vibrational spectral IR intensities and Raman activities of the title compound by DFT method with B3LYP at 6-31G(d,p) and 6-311++G(d,p) basis sets have been collected

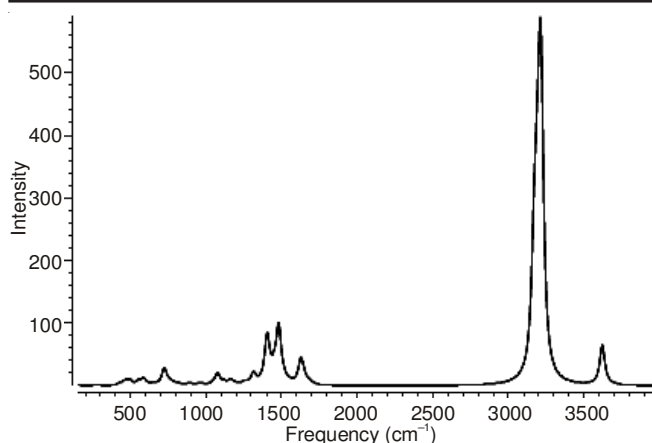


Fig. 5. Comparative graph of calculated FT-Raman spectrum

in Table-4. The title molecule is a non-polar and belongs to C₁ point group. Comparison of IR intensity and raman activity are calculated by B3LYP with 6-31G(d,p) and 6-311G(d,p) basis sets. In the case of IR intensity and Raman activity, the values by B3LYP/6-311++G(d,p) are found to be higher than B3LYP at 6-31G(d,p) levels.

CH vibrations: The existence of one or more aromatic rings in a structure is normally readily determined from the C-H and C-C ring related vibrations. The substituted benzene like molecule gives rise to C-H stretching, C-H in-plane and C-H out-of-plane bending vibrations. The hetro aromatic structure shows the presence of C-H stretching vibration in the region 3100-3000 cm⁻¹, which is the characteristic region for the ready identification of C-H stretching vibration^{19,20}. In this region, the bands are not affected appreciably by the nature of the substituent. The aromatic C - H stretching frequencies arise from the modes observed at 3062, 3047 cm⁻¹ and 3080 cm⁻¹ of benzene and its derivatives²¹. In our present work, the C-H stretching vibrations are observed at 3131, 3090 and 3050 cm⁻¹ in FT-IR and at 3066 cm⁻¹ in FT-Raman spectrum for C-H vibrations. The calculated values of these modes for the title molecule have been found to be 3094, 3063 and 3046 at B3LYP calculation level. As indicated by the potential energy distribution, these four modes involve approximately 99 % contribution suggesting that they are pure stretching modes.

The aromatic C-H in-plane bending modes of benzene and its derivatives are observed in the region 1300-1000 cm⁻¹²². The C-H in plane bending vibrations are identified at 1626, 1510, 1449, 1228, 1053 cm⁻¹ in FT-IR and at 1630, 1514, 1040 cm⁻¹ in FT-Raman spectrum. The aromatic C-H in-plane bending vibrations have substantial overlapping with the ring C-C stretching vibrations. The absorption bands arising from C-H out-of-plane bending vibrations are usually observed in the region at 1000-675 cm⁻¹²³. The C-H out-of-plane bending vibrations are observed as strong bands in FTIR at 984, 899, 874, 778 cm⁻¹ and Raman active mode can be observed as medium bands in Raman spectrum at 890, 716 cm⁻¹. The HCH, HCC bending vibrations are observed in both spectra with 75 % of potential energy distribution contribution. This also shows good agreement with theoretically scaled harmonic wave number values.

CC vibrations: The carbon-carbon stretching modes of the phenyl group are expected in the range from 1650 to 1200

TABLE-4
COMPARATIVE VALUES OF IR INTENSITY AND RAMAN ACTIVITY BETWEEN B3LYP/6-31G(d,p) AND B3LYP/6-311G(d,p) OF HYDROXYBENZOPYRIDINE

S. No.	Calculated with B3LYP/6-31G(d,p)		Calculated with B3LYP/6-311++G(d,p)	
	^a IR intensity	^b Raman activity	^a IR intensity	^b Raman activity
1	0.09	1.43	0.14	0.740
2	1.91	0.03	2.97	0.05
3	0.79	1.30	1.73	0.93
4	4.62	0.94	3.95	1.11
5	0.75	3.05	1.95	0.86
6	11.07	6.63	12.10	7.45
7	0.02	0.65	0.02	0.08
8	0.17	6.50	0.07	6.68
9	3.50	5.20	3.59	5.11
10	0.71	7.73	0.88	9.66
11	0.57	2.52	5.42	0.04
12	31.04	0.71	85.90	0.78
13	78.31	2.46	11.05	0.41
14	17.39	27.45	18.63	33.44
15	17.50	3.82	23.36	0.48
16	9.24	1.99	29.45	0.24
17	2.75	1.77	2.90	2.34
18	43.80	0.18	52.59	0.17
19	0.92	2.69	0.61	0.70
20	1.75	1.15	2.06	2.33
21	0.24	2.62	0.01	0.15
22	0.35	1.11	0.27	0.47
23	0.72	0.06	0.74	0.23
24	0.17	3.12	0.95	3.87
25	3.40	17.55	3.62	26.24
26	16.46	3.47	24.74	6.75
27	0.51	8.14	0.66	4.99
28	165.50	1.42	16.93	1.85
29	40.07	1.27	40.50	2.94
30	38.14	3.25	53.63	6.70
31	22.75	7.78	50.99	14.68
32	122.53	9.11	75.81	7.67
33	42.42	72.17	23.51	90.37
34	37.84	4.32	45.41	14.33
35	34.97	15.39	38.86	18.13
36	10.51	90.76	4.73	102.55
37	70.59	3.70	85.22	3.45
38	138.33	1.87	128.41	3.50
39	24.12	38.73	24.5	45.97
40	6.57	7.53	8.31	7.85
41	9.53	4.66	8.65	5.21
42	22.06	138.38	16.29	135.85
43	6.96	15.74	6.58	35.30
44	3.16	114.41	1.77	99.60
45	22.62	137.58	17.89	128.82
46	18.74	213.98	15.55	224.55
47	7.52	213.49	5.59	241.95
48	92.63	63.45	104.26	65.45

^aRelative absorption intensities normalized with highest peak absorption equal to 100, ^bRelative Raman activities normalized to 100.

cm⁻¹. The actual position of these modes is determined not so much by the nature of the substituents but by the form of substitution around the ring. In general, the bands are of variable intensity and are observed at 1625-1590, 1590-1575, 1540-1470, 1465-1430 and 1380-1280 cm⁻¹ from the wave number ranges given by Varsanyi²⁴ for the five bands in the region. In

the present work, the wave numbers observed in the FTIR spectrum at 1350, 1275, 1170 cm^{-1} in FT-IR spectrum and in FT-Raman spectrum at 1275, 1226, 1185 cm^{-1} have been assigned to C-C stretching vibrations. The theoretically computed values at 1361, 1266 and 1192 cm^{-1} show an excellent agreement with experimental data. These modes are mixed mode with the contribution of C-H in-plane bending vibration in this region and the modes are confirmed by the potential energy distribution values as shown in Table-3.

The aromatic C-H in-plane bending modes of benzene and its derivatives are observed in the region 1300-1000 cm^{-1} . The C-C-C out-of-plane bending modes are observed at 865, 819 cm^{-1} and these wave numbers are consistent with the theoretical wave numbers. The C-C stretching vibrations are attributed to the low wave numbers at 1059 cm^{-1} in FT-IR and at 1053, 1040, 1012, 1003, 958, 734 cm^{-1} in FT-Raman spectrum. The same vibrations are predicted for 1-azanaphthalene-8-ol. at 1093, 1057, 889 and 783 cm^{-1} by B3LYP methods. The C-C-C in-plane and out-of-plane bending vibrations are also computed theoretically and the correlation between the experimental and theoretical values are observed.

CN vibrations: In aromatic compounds, the CN stretching vibrations usually in the region 1400-1200 cm^{-1} . The identification of CN stretching frequencies was a rather difficult task since the mixing of vibrations was possible in this region^{25,26}. In this study, the bands observed at 1478, 1350 and 1275 cm^{-1} in FT-IR spectrum and 1185 cm^{-1} in Raman spectrum have been assigned to CN stretching vibrations of the title compound. The in-plane and out-of plane bending CN vibrations had also been identified and presented in Table-4.

Natural bond orbital (NBO) analysis: NBO analysis provides an efficient method for studying intra and intermolecular bonding and interaction among bonds and also provides a convenient basis for investigation charge transfer or conjugative interactions in molecular system²⁷. Some electron donor orbital, acceptor orbital and the interacting stabilization energy resulting from the second order micro-disturbance theory are reported^{28,29}. The larger the $E(2)$ value, the more intensive is the interaction between electron donors and the greater the extent of conjugation of the whole system. Delocalization of electron density between occupied Lewis type (bond or lone pair) NBO orbitals and formally unoccupied (antibonding or

Rydberg) non Lewis NBO orbital's correspond to a stabilizing donor-acceptor interaction. Natural bond orbital analysis performed on the molecule at the DFT/B3LYP/6-31G(d,p) level in order to elucidate the intra molecular rehybridization and delocalization of electron density within the molecule. The molecular interaction is formed by the orbital overlap between $\sigma(\text{C-C})$ and $\sigma^*(\text{C-C})$ bond orbital which results intramolecular charge (ICT) causing stabilization of the system. These interactions are observed as increase in electron density (ED) in C-C antibonding orbital that weakens the respective bonds. The electron density of conjugated double as well as the single bond of the conjugated ring (-1.9 e) clearly demonstrates strong delocalization inside the molecule.

Natural bond orbital analysis stresses the role of intermolecular orbital interaction in the complex, particularly charge transfer. This is carried out by considering all possible interactions between filled donor and empty acceptor NBOs and estimating their energetic importance by second-order perturbation theory. For each donor NBO (i) and acceptor NBO (j), the stabilization energy $E^{(2)}$ associated with electron delocalization between donor and acceptor is estimated as:

$$E^{(2)} = q_i \frac{(F_{i,j})^2}{\epsilon_j - \epsilon_i}$$

where q_i is the orbital occupancy, ϵ_i , ϵ_j are diagonal elements and $F_{i,j}$ is the off-diagonal NBO Fock matrix element.

Table-5 lists the calculated occupancies of natural orbital's. Three classes of NBOs are included, the Lewis-type (σ and π bonding or lone pair) orbital's, the valence non-Lewis (acceptors formally unfilled) orbital's and the Rydberg NBOs, which originate from orbitals outside the atomic valence shell. The calculated natural hybrids on atoms are also given in this Table-5. As seen from the Table-5, the $\sigma(\text{N1-C10})$ bond is formed from and $sp^{1.57}$ hybrid on nitrogen (which is the mixture of 38.81 %s, 60.99 %p and 0.20 %d atomic orbital's). On the other hand $s(\text{N1-C2})$ bond is formed from a $sp^{1.64}$ hybrid on nitrogen (which is the mixture of 37.80 %s, 61.98 %p and 0.22 %d orbitals). The $\pi(\text{C9-O11})$ is formed from an $sp^{3.12}$ hybrid on oxygen (which is the mixture of 24.21 %s, 75.60 %p and 0.18 %d).

In Table-6, the perturbation energies of donor-acceptor interactions are presented. In our title molecule hydroxybenzo-

TABLE-5
OCCUPANCY OF NATURAL ORBITALS (NBOS) AND HYBRIDS OF HYDROXYBENZOPYRIDINE
CALCULATED BY B3LYP METHOD WITH 6-31G(d,p) BASIS SET

Donor Lewis-type NBOs	Occupancy	Hybrid	AO (%)
$\sigma\text{N1-C2}$	1.9828	$sp^{1.64}$	s (37.80), p (60.99), d (0.22)
$\sigma\text{N1-C10}$	1.9744	$sp^{1.57}$	s (38.81), p (60.99), d (0.20)
$\sigma\text{C2-C3}$	1.9751	$sp^{1.65}$	s (37.65), p (62.29), d (0.05)
$\sigma\text{C9-O11}$	1.9922	$sp^{3.12}$	s (24.21), p (75.60), d (0.18)
$\sigma\text{O11-H18}$	1.9909	$sp^{3.02}$	s (24.89), p (75.06), d (0.05)
LP(1)N1	1.8923	$sp^{3.35}$	s (22.93), p (76.88), d (0.19)
LP(1)O11	1.9771	$sp^{1.67}$	s (37.44), p (62.50), d (0.06)
$\sigma^*\text{N1-C2}$	0.0160	$sp^{1.64}$	s (37.80), p (61.98), d (0.22)
$\sigma^*\text{C2-C3}$	0.0310	$sp^{1.65}$	s (37.65), p (62.29), d (0.05)
$\sigma^*\text{C2-H12}$	0.0309	$sp^{2.33}$	s (30.02), p (69.95), d (0.03)
$\sigma^*\text{C9-O11}$	0.0252	$sp^{3.12}$	s (24.21), p (75.60), d (0.18)
$\sigma^*\text{O11-H18}$	0.0146	$sp^{3.02}$	s (24.89), p (75.06), d (0.05)

pyridine $\pi(\text{C3-C4}) \rightarrow \pi^*(\text{N1-C2})$ has 28.18 kJ/mol, $\pi(\text{C8-C9}) \rightarrow \pi^*(\text{C6-C7})$ has 19.68 kJ/mol and $\pi(\text{C6-C7}) \rightarrow \pi^*(\text{C8-C9})$ has 14.11 kJ/mol and hence they give stronger stabilization to the structure. Table-6 showed that the maximum occupancies 1.98282, 1.97443, 1.97506, 1.97556 are obtained for $\sigma(\text{N1-C2})$, $\sigma(\text{N1-C10})$, $\sigma(\text{C2-C3})$ and $\pi(\text{C6-C7})$, respectively. Therefore the results suggest that the $\sigma(\text{N1-C2})$, $\sigma(\text{N1-C10})$, $\sigma(\text{C2-C3})$ and $\pi(\text{C6-C7})$ are essentially controlled by the p -character of the hybrid orbital's.

The same kind of interaction is calculated in the same kind of interaction energy, related to the resonance in the molecule, is electron donating from LP(1) C10 to $\sigma^*(\text{C2-C3})$ shows less stabilization of 10.44 kJ/mol and further LP(1)C10 to $\pi^*(\text{N1-C2})$ leads to strong stabilization energy of 81.91 kJ/mol and LP(1)C10 to $\pi^*(\text{C8-C9})$ resulting in an enormous stabilization of 83.18 kJ/mol. The strong intra-molecular hyper conjugation interaction of the σ and the π electrons of C-C to the anti C-C bond in the ring leads to stabilization of some part of the ring as evident from the Table-6.

Frontier molecular orbital analysis: The HOMO (highest occupied molecular orbital)-LUMO (lowest unoccupied molecular orbital) energy gap of hydroxybenzopyridine has been calculated at the B3LYP/6-31G(d,p). Many organic molecules containing π conjugated electrons are characterized hyperpolarizabilities and were analyzed by means of vibrational spectroscopy^{30,31}. These orbitals determine the way the molecule interacts with other species. Fig. 6 shows the distributions and energy levels of the HOMO-1, HOMO, LUMO and LUMO+1 orbitals computed at the B3LYP/6-31G(d,p) level for the title compound. The calculated energy values are presented

in Table-7. HOMO is mainly localized on the hydroxyl group and LUMO is delocalized over the entire molecule. HOMO-1 is delocalized over the entire molecule and LUMO+1 is localized on the hydroxyl group and methyl group. The value of the energy separation between the HOMO and LUMO is 0.15698 a.u. The lowering of the HOMO-LUMO band gap is essentially a consequence of the large stabilization of the LUMO due to the strong electron-acceptor ability of the electron-acceptor group. The higher the energy of HOMO, the easier it is for HOMO to donate electrons whereas it is easier for LUMO to accept electrons when the energy of LUMO is low. Moreover lower in the HOMO-LUMO energy gap explains the eventual charge transfer interactions taking place within the molecule.

TABLE-7
HOMO-LUMO ENERGY VALUE OF HYDROXYBENZOPYRIDINE CALCULATED BY B3LYP METHOD WITH 6-31G(d,p), 6-311++G(d,p) BASIS SETS

Parameters	B3LYP/ 6-31G(d,p) (a.u)	B3LYP/ 6-311++G(d,p) (a.u)
E_{HOMO} (a.u)	-0.21022	-0.22485
E_{LUMO} (a.u.)	-0.05324	-0.06978
$\Delta E_{\text{HOMO-LUMO gap}}$ (a.u)	0.15698	0.15507
$E_{\text{HOMO-1}}$ (a.u.)	-0.2547	-0.26749
$E_{\text{LUMO+1}}$ (a.u.)	-0.01847	-0.03572
$\Delta E_{\text{HOMO-1-LUMO+1 gap}}$ (a.u)	0.23623	0.23177

Mulliken atomic charges: Mulliken atomic charges calculation has an important role in the application of quantum chemical calculation to molecular system because atomic charges affect dipole moment, molecular polarizability, elec-

TABLE-6
SECOND ORDER PERTURBATION THEORY ANALYSIS OF FOCK MATRIX IN NBO BASIS IN HYDROXYBENZOPYRIDINE

Donor (i)	Type	ED(e)	Acceptor(j)	Type	ED(e)	$E(2)^a$ (kJ/mol)	$E(j)-E(i)^b$ (a.u.)	$F(i, j)^c$ (a.u.)
N1-C2	σ	1.98281	N1-C10	σ^*	0.02616	3.02	1.56	0.061
			C2-C3	σ^*	0.03097	1.99	1.51	0.049
			C9-C10	σ^*	0.03088	5.17	1.54	0.080
N1-C2	σ	1.82390	C3-C4	σ^*	0.19090	8.50	0.39	0.052
			C5-C10	σ^*	0.05370	0.52	0.99	0.021
N1-C10	σ	1.97443	N1-C2	σ^*	0.01605	2.85	1.54	0.059
			C5-C10	σ^*	0.05370	4.45	1.55	0.075
C2-C3	σ	1.97506	N1-C2	σ^*	0.01605	2.20	1.40	0.050
			C4-C14	σ^*	0.02375	5.29	1.16	0.070
C2-H12	σ	1.97053	N1-C10	σ^*	0.02616	5.01	1.21	0.070
			C3-C4	π^*	0.19090	3.82	0.59	0.044
C3-C4	σ	1.96835	C2-C3	σ^*	0.03097	4.48	1.44	0.072
C3-C4	π	1.69240	N1-C2	π^*	0.1605	28.18	0.33	0.086
C3-H13	σ	1.97102	C2-H2	σ^*	0.03127	0.57	0.73	0.020
			C4-C5	σ^*	0.03127	4.13	1.16	0.062
C4-C5	σ	1.95722	C3-H13	σ^*	0.02555	7.02	1.14	0.080
C4-H14	σ	1.96774	C5-C10	σ^*	0.05370	4.83	1.20	0.068
C5-C6	σ	1.95703	C6-C7	σ^*	0.01691	4.07	1.39	0.068
C6-C7	π	1.97566	C8-C9	π^*	0.33166	14.11	0.32	0.061
C8-C9	π	1.97178	C6-C7	π^*	0.29364	19.68	0.31	0.070
			C2-C3	σ^*	0.03097	10.44	0.97	0.091
C10	LP(1)	1.0388	N1-C2	π^*	0.32514	81.91	0.13	0.113
			C8-C9	π^*	0.33166	83.18	0.16	0.123
O11	LP(2)	1.86739	C8-C9	π^*	0.33166	30.01	0.36	0.098

^a $E(2)$ means energy of hyper conjugative interaction (stabilization energy), ^bEnergy difference between donor and acceptor i and j NBO orbitals, ^c $F(i, j)$ is the Fock matrix element between i and j NBO orbitals

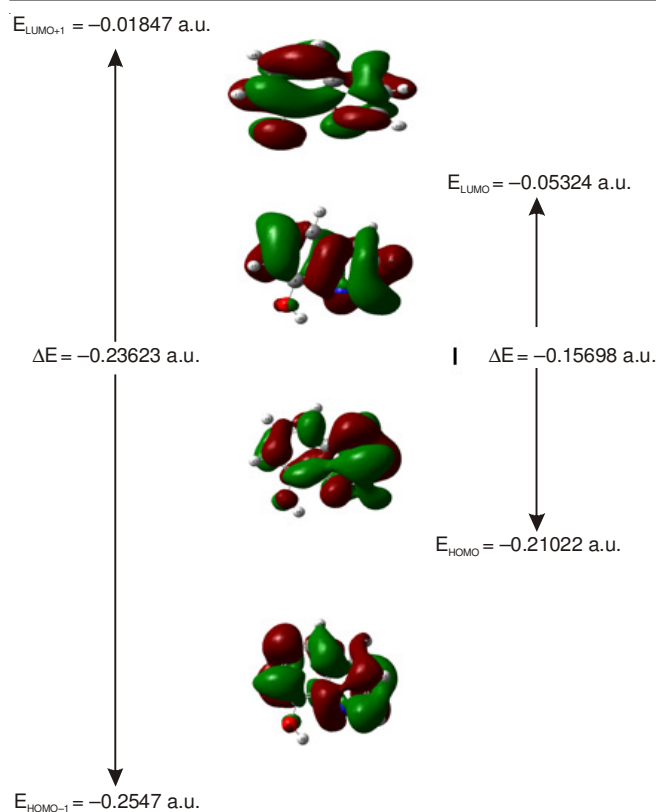


Fig. 6. Atomic orbital composition of the frontier molecular orbital of hydroxybenzopyridine

tronic structure and a number of properties of molecular systems³². The charge distribution over the atoms suggests the formation of donor and acceptor pairs involving the charge transfer in the molecule. Atomic charge has been used to describe the processes of electro-negativity equalization and charge transfer in chemical reactions^{33,34}. Mulliken atomic charges calculated by methods B3LYP/6-31G(d,p) and B3LYP/cc-pVDZ methods are collected in Table-8. It is worthy to mention that C2, C5 and C10 atoms of the title molecule exhibit positive charge while C3, C4, C6, C7, C8, C9 atoms exhibit negative charges. Oxygen has a maximum negative charge value of about -0.5888 in the OH group. The maximum positive atomic is obtained for C10 which is a carbon present in the CN functional group. The charge on H18 in the functional group has the maximum magnitude of 0.3275 among the hydrogen atoms present in the molecule at 6-31G(d,p) and cc-pVDZ level of theory. However all the hydrogen atoms exhibit a net positive charge in 6-31G(d,p) basis set while all hydrogen atoms possess negative charge. The presence of large negative charge on

O and N atom and net positive charge on H atom may suggest the formation of intermolecular interaction in solid forms³⁵.

Other molecular properties

Analysis of molecular electrostatic potential (MESP): Molecular electrostatic potential (MEP) at a point in the space around a molecule gives an indication of the net electrostatic effect produced at that point by the total charge distribution (electron + nuclei) of the molecule and correlates with dipole moments, electronegativity, partial charges and chemical reactivity of the molecules^{36,37}. It provides a visual method to understand the relative polarity of the molecule. The different values of the electrostatic potential represented by different colors; red represents the regions of the most negative electrostatic potential, white represents the regions of the most positive electrostatic potential and blue represents the region of zero potential. Potential increases in the order red < green < blue < pink < white. It can be seen that the negative regions are mainly over the O11 atom. The negative (red colour) regions of molecular electrostatic potential were related to electrophilic reactivity and the positive (white colour) ones to nucleophilic reactivity. The negative electrostatic potential corresponds to an attraction of the proton by the aggregate electron density in the molecule (shades of red), while the positive electrostatic potential corresponds to the repulsion of the proton by the atomic nuclei (shades of white) According to these calculated results, the molecular electrostatic potential map shows that the negative potential sites are on oxygen atoms as well as the positive potential sites are around the hydrogen atoms. These sites give information concerning the region from where the compound can have metallic bonding and intermolecular interactions. The predominance of light green region in the molecular electrostatic potential surfaces corresponds to a potential halfway between the two extremes red and dark blue colour. The total electron density and molecular electrostatic potential surfaces of the molecules under investigation are constructed by using B3LYP/6-31G(d,p) method. These pictures illustrate an electrostatic potential model of the compounds, computed at the 0.002 a.u. isodensity surface. The molecular electrostatic potential mapped surface of the compounds and electrostatic potential map for positive and negative potentials is shown in Fig. 7. The molecular electrostatic potential map shows that the negative potential sites are on electronegative atoms as well as the positive potential sites are around the hydrogen atoms. These sites give information about the region from where the compound can have non covalent interactions.

TABLE-8
MULLIKEN ATOMIC CHARGES CALCULATED BY B3LYP/6-31G (d,p) AND B3LYP/cc-pVDZ METHODS

Atomic No	B3LYP/6-31G(d,p)	B3LYP/cc-pVDZ	Atomic No	B3LYP/6-31G(d,p)	B3LYP/cc-pVDZ
N1	-0.5093	-0.1535	C10	0.2566	0.1038
C2	0.0788	0.0576	O11	-0.5889	-0.1829
C3	-0.1245	-0.0056	H12	0.0976	-0.0147
C4	-0.0849	0.0789	H13	0.0966	-0.0170
C5	0.1559	0.0739	H14	0.1145	-0.0106
C6	-0.1565	-0.0199	H15	0.0681	-0.0640
C7	-0.0990	0.0546	H16	0.0862	-0.0285
C8	-0.1432	0.0348	H17	0.0908	-0.0305
C9	0.3337	-0.0198	H18	0.3275	0.1434

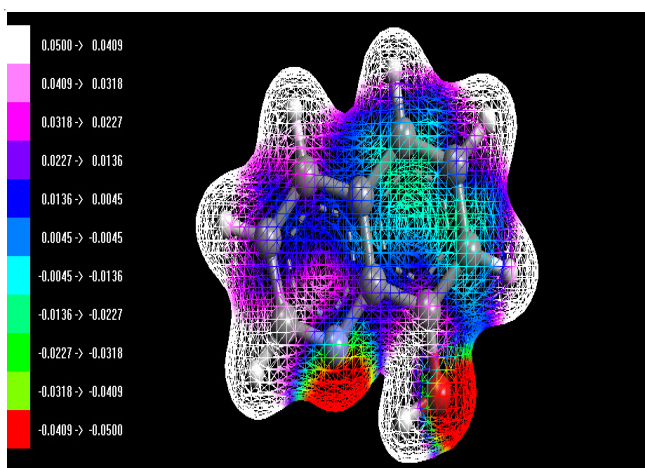


Fig. 7. Molecular electrostatic potential map of hydroxybenzopyridine

First order hyperpolarizability calculations: Polarizabilities and hyperpolarizabilities characterize the response of a system in an applied electric field³⁸. They determine not only the strength of molecular interactions as well as the cross sections of different scattering and collision processes, but also the non-linear optical properties (NLO) of the system^{39,40}. In order to investigate the relationships among photocurrent generation, molecular structures and NLO, the polarizabilities and hyperpolarizabilities of title compound was calculated using B3LYP method, 6-31G(d,p) basis set, based on the finite-field approach. The first order hyperpolarizability (β) of title molecule along with related properties (μ , α and α_0) are reported in Table-9. The calculated value of dipole moment was found to be 1.03354 Debye at B3LYP/6-31G(d,p). In addition to the isotropic polarizabilities and polarizabilities anisotropy invariant were also calculated. The calculated anisotropy of the polarizability α of hydroxybenzopyridine is 249.8787 a.u at B3LYP/6-31G(d,p) level. The magnitude of the molecular hyperpolarizability β , is one of key factors in a NLO (non-linear optical) system. The B3LYP/6-31G(d,p) calculated first order hyperpolarizability value (β_0) of hydroxybenzopyridine is equal to 2.4302×10^{-30} esu. Total dipole moment of title molecule is slightly smaller than those of urea and first order hyperpolarizability of title molecule is approximately

Parameters	B3LYP/6-31G(d,p)	Parameters	B3LYP/6-31G(d,p)
μ_x	0.70363	β_{xxx}	153.85928
μ_y	-0.74025	β_{xyy}	0.715038
μ_z	-0.15871	β_{xyy}	16.87299
μ	1.03354	β_{yyv}	-186.3781
α_{xx}	136.04879	β_{xxz}	-33.5478
α_{xy}	0.126794	β_{xyz}	26.81478
α_{yy}	104.51901	β_{yyz}	25.29785
α_{xz}	-3.49817	β_{zzz}	18.6219
α_{yz}	-2.60709	β_{yzz}	-20.5898
α_{zz}	41.75965	β_{zzz}	-18.7576
α_0	94.1091	β_{tot} (esu)	2.4302×10^{-30}
α	249.8787	-	-

eight times greater than those of urea. This result indicates the nonlinearity of the title molecule.

Fukui functions: DFT is one of the important tools of quantum chemistry to understand popular chemical concepts such as electro negativity, electron affinity, chemical potential and ionization potential. In order to solve the negative Fukui function problem, different attempts have been made by various groups⁴¹. Kollandaivel *et al.*⁴² introduced the atomic descriptor to determine the local reactive sites of the molecular system. In the present study, the optimized molecular geometry was utilized in single-point energy calculations, which have been performed at the DFT for the anions and cations of the title compound using the ground state with doublet multiplicity. The individual atomic charges calculated by natural population analysis (NPA) and Mulliken population analysis (MPA) have been used to calculate the Fukui function. Table-10 shows the f_k^+ , f_k^- and f_k^0 values for the title molecule calculated by NPA and MPA gross charges at DFT level of theory with the basis set (B3LYP/6-31G(d,p)). It has been found that both NPA and MPA scheme methods predict that the nitrogen atom N1 has a higher f_k^+ value for nucleophilic attack. Also both the population analysis schemes show N1 nitrogen atom as the reactive sites for receiving a nucleophilic. From the values reported in the Table-10 the reactivity order for the electrophilic case was C9>C4>C3 for MPA analysis. On the other hand for nucleophilic attack both N1 and O11 has greater reactivity value. The attack for radical case was C10 > C4 for MPA. If one compares the three kinds of attacks, it is possible to observe that the electrophilic attack has bigger reactivity compared to the nucleophilic and radial attack.

Thermodynamic properties: All the thermodynamic data provide helpful information for the study of thermodynamic energies and estimate directions of chemical reactions according to the second law of thermodynamics in thermo chemical field⁴³. The thermodynamic parameters such as zero-point vibrational energy, thermal energy, rotational constants, entropy and dipole moment of title molecule are calculated by B3LYP method using 6-31G(d,p),6-311++G(d,p) basis sets. Scale factors have been recommended^{44,45} for an accurate prediction in determining the Zero-Point Vibration Energies (ZPVE) and the entropy, the variations in the ZPVEs seems to be significant. Table-11 demonstrates several thermodynamic parameters of the title compound without of results of experimental. The smallest value of ZPVE is 87.7700 Kcal/mol obtained at B3LYP/6-311++G(d,p) whereas the biggest value is 88.09584 Kcal/mol, 88.34190 Kcal/mol obtained for B3LYP/cc-pVDZ, B3LYP/6-31G(d,p), respectively. The total energies are found to decrease with the increase of the basis set dimension and the change in the Gibbs free energy of title compound at room temperature with different basis set are only marginal. The dipole moment of the molecule was also calculated by B3LYP method with 6-31G(d,p),6-311++G(d,p) and cc-pVDZ basis sets. Dipole moment reflects the molecular charge distribution and is given as a vector in three dimensions. Therefore, it can be used as descriptor to depict the charge movement across the molecule depends on the centers of positive and negative charges. Dipole moments are strictly determined for neutral molecules. For charged systems, its value depends on the choice of origin and molecular orientation. As a result of B3LYP

TABLE-10
CONDENSED FUKUI FUNCTIONS CALCULATED BY B3LYP/6-31G(d,p) FROM THE NPA AND MPA SCHEMES

Atoms	MPA			NPA		
	$f k^+$	$f k^-$	$f k^0$	$f k^+$	$f k^-$	$f k^0$
N1	0.4701	-0.3344	0.0679	0.0852	0.1005	0.0929
C2	-0.1407	-0.5256	-0.3332	0.0626	-0.0167	0.0230
C3	0.0174	0.1277	0.0726	0.1093	0.0964	0.1029
C4	0.0147	0.6649	0.3398	0.0804	0.1471	0.1138
C5	1.1193	-2.5394	-0.7101	-0.0194	-0.0190	-0.0192
C6	-0.1619	-0.0423	-0.1021	0.2147	-0.0137	0.1005
C7	-0.1780	-0.0936	-0.1358	0.0552	0.0043	0.0298
C8	0.3466	-0.1646	0.0910	0.1439	0.0204	0.0822
C9	-0.8558	0.8845	0.0144	0.0872	0.0322	0.0597
C10	-1.0076	2.0707	0.5316	-0.0185	0.0315	0.0065
O11	0.4396	-0.2676	0.0860	0.1400	0.0104	0.0752
H12	0.1636	0.6069	0.3853	0.0032	0.1731	0.0882
H13	0.1403	0.3654	0.2529	0.0127	0.1262	0.0695
H14	0.1416	0.1849	0.1633	0.0108	0.0942	0.0525
H15	0.1586	-0.0032	0.0777	0.0059	0.0568	0.0314
H16	0.1535	0.0014	0.0775	0.0079	0.0636	0.0358
H17	0.1780	-0.0214	0.0783	0.0110	0.0600	0.0355
H18	0.0004	0.0857	0.0431	0.0076	0.0327	0.0202

TABLE-11
THERMODYNAMIC PARAMETERS OF YDROXYBENZOPYRIDINE ALONG
WITH THE ZERO POINT ENERGY CALCULATED BY B3LYP METHODS

Parameters	3LYP/6 1G(d,p)	B3LYP/6-31++G(d,p)	B3LYP /cc-pVDZ
Zero-point correction	0.1408	0.13987	0.1403
Gibbs free energy	0.1085	0.107545	0.1081
Energy	0.1483	0.14752	0.1479
SCF energy (a.u)	-476.9929	-477.28	-477.19
Nuclear repulsion energy (Hartrees)	557.8688	558.402	557.13
Enthalpy	0.149315	0.148469	0.1489
Total	93.104	92.573	92.847
Translational	0.889	0.889	0.8890
Rotational	0.889	0.889	0.8890
Vibrational	91.329	90.795	91.70
Thermal free energies	-477.0628	-477.179	-477.083

calculations the highest dipole moments were observed for B3LYP/6-311++G(d,p) whereas the smallest one was observed for B3LYP/6-31G(d,p) in the title compound.

Conclusion

The FT-IR and FT-Raman have been recorded and the detailed vibrational assignment is presented for hydroxybenzopyridine. A complete vibrational investigation of hydroxybenzopyridine has been performed using FT-IR and Raman spectroscopic techniques and the various modes of vibrations were explicitly assigned on the results of potential energy distribution output obtained from the normal coordinate analysis. The equilibrium geometries, harmonic frequencies and infrared intensities of the molecule were determined and analyzed by B3LYP with 6-31G(d,p) basis sets. The simulated FT-IR and Raman spectra of hydroxybenzopyridine show good agreement with the observed spectra. The difference between the observed and scaled wave number values of the most of the fundamental is very small. Therefore the assignments with reasonable deviation from the experimental value seem to be correct. This study demonstrates that scaled DFT (B3LYP) calculations are powerful approach for understanding the vibrational spectra of hydroxybenzopyridine. The molecular Gibbs's free energy, the reaction enthalpy and several thermo dynamical parameters

were also being found with the *ab initio* HF and DFT methods. The predicted first hyperpolarizability shows that the molecule might have a reasonably good nonlinear optical (NLO) behaviour. Mulliken atomic charge analysis shows that charge transfer occurring within the molecule. NBO results reflects the charge transfer mainly due to C-O group. The natural bond orbital (NBO) analysis has provided the detailed insight into the type of hybridization and the nature of bonding in hydroxybenzopyridine. The σ (N1-C2) bonds are formed from an $sp^{1.64}$ hybrid on nitrogen atom and π (C9-O11) bond is formed from an $sp^{3.12}$. The strongest electron donation occurs from a lone pair to the anti-bonding acceptor π^* (C8-C9) orbital's. Increased HOMO and LUMO energy gap explains the eventual charge transfer within the molecule which is responsible for the chemical reactivity of the molecule.

REFERENCES

1. G. Collin and H. Höke, Quinoline and Isoquinoline, Ullmann's Encyclopedia of Industrial Chemistry, Weinheim: Wiley-VCH (2005).
2. J.P. Phillips, *Chem. Rev.*, **56**, 271 (1956).
3. R. Katakura and Y. Koide, *Inorg. Chem.*, **45**, 5730 (2006).
4. K.G. Stone and L. Friedman, *J. Am. Chem. Soc.*, **69**, 209 (1947).
5. M. Santo, R. Cattana and J.J. Silber, *Spectrochim. Acta A*, **57**, 1541 (2001).

6. C. Reichardt, Solvents and Solvent Effects in Organic Chemistry, WILEY-VCH Verlag GmbH & Co. KgaA, Weinheim, edn 3 (2003).
7. Z. Zhou, D. Du, Y. Xing and S.U.M. Khan, *Mol. J. Struct. (Theochem)*, **505**, 247 (2000).
8. Z. Zhou, A. Fu and D. Du, *Int. J. Quantum Chem.*, **78**, 186 (2000).
9. Z. Zhou, A. Fu and D. Du, *Int. J. Quantum Chem.*, **78**, 186 (2000).
10. D.C. Young, Computational Chemistry: A Practical Guide for Applying Techniques to Real World Problems (Electronic), John Wiley & Sons Inc, New York (2001).
11. N. Sundaraganesan, S. Ilakiamani, H. Saleem, P.M. Wojciechowski and D. Michalska, *Spectrochim. Acta A*, **61**, 2995 (2005).
12. M.J. Frisch, G.W. Trucks, H.B. Schlegel, G.E. Suzerain, M.A. Robb, J.R. Cheeseman Jr., J.A. Montgomery, T. Vreven, K.N. Kudin, J.C. Burant, J.M. Millam, S.S. Iyengar, J. Tomasi, V. Barone, B. Mennucci, M. Cossi, G. Scalmani, N. Rega, G.A. Petersson, H. Nakatsuji, M. Hada, M. Ehara, K. Toyota, R. Fukuda, J. Hasegawa, M. Ishida, T. Nakajima, Y. Honda, O. Kitao, H. Nakai, M. Klene, X. Li, J.E. Knox, H.P. Hratchian, J.B. Cross, V. Bakken, C. Adamo, J. Jaramillo, R. Gomperts, R.E. Stratmann, O. Yazyev, A.J. Austin, R. Cammi, C. Pomelli, J.W. Ochterski, P.Y. Ayala, K. Morokuma, G.A. Voth, P. Salvador, J.J. Dannenberg, V.G. Zakrzewski, S. Dapprich, A.D. Daniels, M.C. Strain, O. Farkas, D.K. Malick, A.D. Rabuck, K. Raghavachari, J.B. Foresman, J.V. Ortiz, Q. Cui, A.G. Baboul, S. Clifford, J. Cioslowski, B. Stefanov, G. Liu, A. Liashenko, P. Piskorz, I. Komaromi, R.L. Martin, D.J. Fox, T. Keith, M.A. Al-Laham, C.Y. Peng, A. Nanayakkara, M. Challacombe, P.M.W. Gill, B. Johnson, W. Chen, M.W. Wong, C. Gonzalez and J.A. Pople, Gaussian 03, Revision A.I, Gaussian, Inc, Pittsburgh, PA (2003).
13. P.C. Hariharan and J.A. Pople, *Theor. Chim. Acta*, **28**, 213 (1973).
14. P.C. Hariharan and J.A. Pople, *Mol. Phys.*, **27**, 209 (1974).
15. A.D. Becke, *J. Chem. Phys.*, **98**, 5648 (1993).
16. A.E. Reed, L.A. Curtiss and F. Weinhold, *Chem. Rev.*, **88**, 899 (1988).
17. J.H. Rodriguez, D.E. Wheeler and J.K. McCusker, *J. Am. Chem. Soc.*, **120**, 12051 (1998).
18. U. Rani, M. Karabacak, O. Tandriverdi, M. Kurt and N. Sundaraganesan, *Spectrochim. Acta A*, **92**, 67 (2012).
19. V.K. Rastogi, M.A. Palafox, R.P. Tanwar and L. Mittal, *Spectrochim. Acta A*, **58**, 1987 (2002).
20. M. Silverstein, G.C. Basseler and C. Morill, Spectrometric Identification of Organic Compounds, Wiley, New York (1981).
21. L.J. Bellamy, The Infrared Spectra of Complex Molecules, Wiley, New York, edn 3 (1975).
22. M. Karabacak, Z. Cinar, M. Kurt, S. Sudha and N. Sundaraganesan, *Spectrochim. Acta A*, **85**, 179 (2012).
23. G. Socrates, Infrared Characteristic Group Frequencies, Wiley-Interscience Publication, New York (1980).
24. G. Varsanyi, Assignments of Vibrational Spectra of Seven Hundred Benzene Derivatives, vols. 1-2, Adam Hilger (1974).
25. V. Krishnakumar and V. Balachandran, *Spectrochim. Acta A*, **61**, 1001 (2005).
26. D.N. Sathyanarayana, Vibrational Spectroscopy, Theory and Applications, New Age International Publishers, New Delhi (2004).
27. M. Snehalatha, C. Ravikumar, I.H. Joe, N. Sekar and V.S. Jayakumar, *Spectrochim. Acta A*, **72**, 654 (2009).
28. C. James, A.A. Raj, R. Reghunathan, V.S. Jayakumar and I.H. Joe, *J. Raman Spectrosc.*, **37**, 1381 (2006).
29. K.- Liu, W. Hou, E. Zumbika and Q. Ni, *J. Zhejiang Univ. Sci. B*, **6**, 1182 (2005).
30. Y. Atalay, D. Avci and A. Basoglu, *Struct. Chem.*, **19**, 239 (2008).
31. T. Vijayakumar, I. Hubert Joe, C.P. Reghunadhan Nair and V.S. Jayakumar, *Chem. Phys.*, **343**, 83 (2008).
32. I. Sidir, Y.G. Sidir, M. Kumalar and E. Tasal, *J. Mol. Struct.*, **134**, 964 (2010).
33. K. Jug and Z.B. Maksic, Theoretical Model of Chemical Bonding, Part 3, Springer, Berlin, vol. 29, p. 233 (1991).
34. S. Fliszar, Charge Distributions and Chemical Effects, Springer, New York (1983).
35. L. Xiao-Hong, L. Xiang-Ru and Z. Xian-Zhou, *Comput. Theor. Chem.*, **969**, 27 (2011).
36. S. Sebastian and N. Sundaraganesan, *Spectrochim. Acta A*, **75**, 941 (2010).
37. E. Scrocco and J. Tomasi, *Adv. Quantum Chem.*, **11**, 115 (1978).
38. C.R. Zhang, H.S. Chen and G.H. Wang, *Chem. Res. Chin. Univ.*, **20**, 64 (2004).
39. Y. Sun, X. Chen, L. Sun, X. Guo and W. Lu, *Chem. Phys. Lett.*, **381**, 397 (2003).
40. O. Christiansen, J. Gauss and J.F. Stanton, *Chem. Phys. Lett.*, **305**, 147 (1999).
41. P. Koldaiveil, G. Praveena and P. Selvarengan, *J. Chem. Sci.*, **117**, 591 (2005).
42. R. Kinkar Roy, K. Hirao, S. Krishnamurty and S. Pal, *J. Chem. Phys.*, **115**, 2901 (2001).
43. R. Zhang, B. Du, G. Sun and Y. Sun, *Spectrochim. Acta A*, **75**, 1115 (2010).
44. M. Alcolea Palafox, *Int. J. Quantum Chem.*, **77**, 661 (2000).
45. R. Desiderato, J.C. Terry, G.R. Freemann and H.A. Levy, *Acta Crystallogr. B*, **27**, 2443 (1971).